

APPROACHING THE HARM OF GRADIENT ATTACKS WHILE ONLY FLIPPING LABELS

Anonymous authors

Paper under double-blind review

ABSTRACT

Machine learning systems deployed in distributed or federated environments are highly susceptible to adversarial manipulations, particularly availability attacks—rendering the trained model unavailable. Prior research in distributed ML has demonstrated such adversarial effects through the injection of gradients or data poisoning. In this study, we aim to better understand the potential of weaker (action-wise) adversaries by asking: Can availability attacks be inflicted solely through the flipping of a subset of training labels, without altering features, and under a strict flipping budget? We analyze the extent of damage caused by constrained label flipping attacks against federated learning under mean aggregation—the dominant baseline in research and production. Focusing on a distributed classification problem, (1) we propose a novel formalization of label flipping attacks on logistic regression models and derive a greedy algorithm that is provably optimal at each training step. (2) To demonstrate that availability attacks can be approached by label flipping alone, we show that a budget of only 0.1% of labels at each training step can reduce the accuracy of the model by 6%, and that some models can perform worse than random guessing when up to 25% of labels are flipped. (3) We shed light on an interesting interplay between what the attacker gains from more *write-access* versus what they gain from more *flipping budget*. (4) We define and compare the power of targeted label flipping attack to that of an untargeted label flipping attack.

1 INTRODUCTION AND RELATED WORK

Machine learning systems can become prime targets for adversarial attacks. *Training-phase poisoning attacks* in particular have gained considerable attention as the widespread use of machine learning in critical applications has grown (Awasthi et al. (2017); Zhang et al. (2017); Paudice et al. (2018); Lu et al. (2022); Huang et al. (2011)). In these attacks, an adversary manipulates the training data in order to degrade or control the final trained model. Unlike evasion and backdoor attacks, poisoning requires no control over inference-time input: it suffices to manipulate part of the training set. Among such attacks, *label flipping* stands out for its simplicity: The attacker simply changes the class label of a subset of training points while leaving other aspects of the data intact. This is especially relevant in federated learning situations where features are fixed by upstream data pipelines and the set of possible labels is predefined. For example, a common scenario is when workers are asked to label predefined images, the labels being in a finite set. We address the following question in the context of a classification problem:

Can an attacker severely degrade a model using only label flips on existing data in a convex setting and under budget constraints?

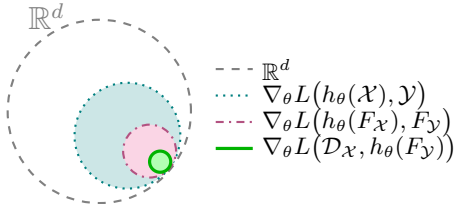


Figure 1: Images of the gradient operator on different sets. \mathbb{R}^d is where an attacker can craft unrestricted gradient attacks. Given a model h_θ , $\nabla_\theta L(h_\theta(\mathcal{X}), \mathcal{Y})$ is the set of possible gradients given an unrestricted data poisoning Bouaziz et al. (2024), $\nabla_\theta L(h_\theta(\mathcal{F}_X), \mathcal{F}_Y)$ is the set of possible gradients when data poisoning is restricted to a feasible set $\mathcal{F}_X \times \mathcal{F}_Y \subseteq \mathcal{X} \times \mathcal{Y}$, and $\nabla_\theta L(\mathcal{D}_X, h_\theta(\mathcal{F}_Y))$ is the set of possible gradients when the features are restricted to those in the dataset \mathcal{D}_X and the labels are chosen in the set of feasible labels.

054
055
056
057
058
059
060
061
062
063
064
065
066
067
068
069
070
071
072
073
074
075
076
077
078
079
080
081
082
083
084
085
086
087
088
089
090
091
092
093
094
095
096
097
098
099
100
101
102
103
104
105
106
107

In this work, we provide a positive answer to this question. By viewing label flipping as a constrained optimization problem from the point of view of the attacker, we show that carefully selected flips can steer the aggregated gradient away from its honest direction and reduce accuracy or render training unstable - even when only 1% of the labels are altered.

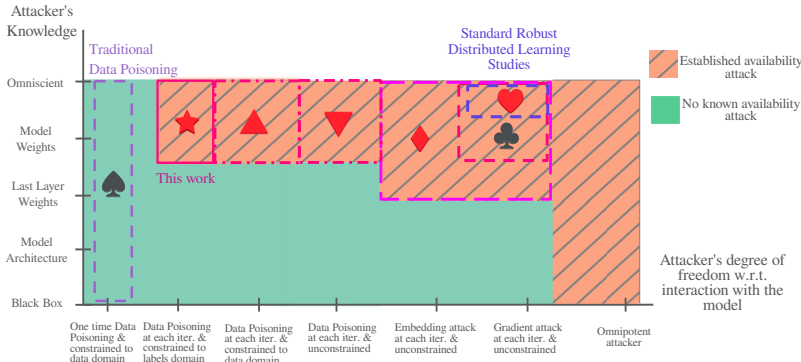


Figure 2: Territory of known availability attacks (in orange) within a domain of constraints. The closer to the origin, the more constrained is the setting for the attacker and the harder it is to realize an availability attack. ♠: Geiping et al. (2020); Zhao & Lao (2022); Ning et al. (2021); Huang et al. (2020), ♥: Blanchard et al. (2017); Baruch et al. (2019), ♣: El-Mhamdi et al. (2018), ◇ so far only in convex settings : Farhadkhani et al. (2022), △&▽ : Bouaziz et al. (2024), ★ : Our contribution in section 3 .

Previous work has investigated poisoning attacks and granted the adversary far more leverage than some realistic scenarios allow. Some require the ability to modify *both* labels and features or even overwrite entire gradients (Bouaziz et al. (2024); Baruch et al. (2019)); others rely on injecting crafted examples into the training set (Shafahi et al. (2018); Zhao & Lao (2022); Koh et al. (2022)). Li et al. (2022) proposes an agglomerative-clustering strategy to select vulnerable samples, assuming access to all training data and performing offline clustering. Jha et al. (2023) demonstrates that carefully chosen label poisoning can insert backdoors via trajectory-matching methods. Their objective is to create targeted misclassification when a trigger is present, not to reduce overall model accuracy. Thus, although both their work and ours manipulate labels only, the goals, threat models, and evaluation metrics differ: theirs aim to insert backdoors, whereas we study availability degradation under a tight budget and online setting. Likewise, Lavaur et al. (2024) applies random label flipping in the context of collaborative intrusion detection systems. The attack of Lavaur et al. (2024) targets domain-specific labels (e.g., DDoS) and does not formalize the attack as an optimization problem. In contrast, we aim to study an attack that is data- and model-agnostic but can be proved to be optimal at each iteration.

Yu et al. (2025) studies label-flipping attacks on GNNs under a federated learning setup. Their approach is oriented towards graph-structured data and relies on the unique properties of GNN aggregation mechanisms. In contrast, we propose a method that is formulated as a general optimization framework based on gradient alignment, making it applicable to a wider range of classification tasks. When manipulation is limited to labels alone, existing methods typically presuppose control over the vast majority of them ($\geq 85\%$) or access to the validation set, and require the training of a number of classifiers linear in the number of classes and the budget (Liu et al. (2023a); Paudice et al. (2018)), unsuitable for online or real-time training, especially at scale.

Another work, Bal et al. (2025), focuses on *defense* in the binary classification setting via adversarial training (SVMs, untargeted), where dual whereas our work formulates the *attacker's* online, budget-constrained optimization and proves per-epoch greedy optimality under explicit write-access and local budget constraints.

By contrast, our work formulates the attacker's optimization problem under a strict, per-epoch budget, with explicit write-access and local budget constraints. Our attack is online, performs per-iteration optimization in parameter space using gradient alignment, and is provably optimal per step. Furthermore, it requires only control over a small fraction of data and changes no features at all,

only labels. This expands the scope of known *availability attacks* to a more limited yet still highly significant threat model.

Following Bouaziz et al. (2024), Figure 2 shows label-flipping attacks on the landscape of availability attacks, situating our contribution within the literature. Meanwhile, Figure 1 illustrates how label flipping compares to more general gradient-based attacks, particularly with respect to the set of gradients achievable under increasingly restrictive conditions.

Why mean aggregation still matters Mean aggregation remains the de facto baseline in both federated learning research and large-scale deployments as it is favored for its scalability, communication efficiency, and ease of implementation (McMahan et al. (2017)). As noted in Shejwalkar et al. (2021), production cross-device FL systems with thousands to billions of clients often employ plain averaging, and empirical evidence suggests that even the most basic, non-robust FL algorithms can be surprisingly resilient in realistic, low-compromise settings. In this context, showing that a constrained, label-flipping adversary can meaningfully degrade model performance under mean aggregation is already a strong and practically relevant finding. Additional discussion is provided in Appendix C.3.

Contributions. We formalize label flipping for logistic regression as a budget-constrained optimization problem whose closed-form objective depends only on the inner products between feature vectors and a reference direction (Section 2). This formulation yields a greedy algorithm that we prove to be *optimal at each training step* (Section 3). Experiments on standard image classification benchmarks confirm the severity of the attack: altering merely 0.1% of the labels already reduces the test accuracy by 6%, a change subtle enough to bypass typical anomaly detection thresholds while still inflicting high computational, financial, and temporal costs. Also, a 25% global budget forces the model to almost random guessing (Section 4). We also discuss the trade-off between an attacker’s *write-access* (k) and their *local budget* (b), showing that a wider write-access is more valuable than a larger local budget, and we compare the targeted and untargeted variants of the proposed algorithm. We then extend the framework to an arbitrary number of classes and propose a generalization of the binary label flipping attack algorithm (Sections 5 and 6). We conclude by discussing limitations of our work and future directions.

2 GENERAL SETTING

2.1 NOTATION

Table 1: Notation Summary

Notation	Description
d	Dimension of the feature space.
t	Epoch (training iteration) index.
(x_n, y_n)	n -th data point, with features $x_n \in \mathbb{R}^{d+1}$ and label $y_n \in \{0, 1\}$.
$\alpha \in \mathbb{R}^{d+1}$	Binary logistic regression parameter vector.
$W \in \mathbb{R}^{C \times (d+1)}$	Multinomial logistic regression parameter matrix.
H	Set of <i>honest</i> data points (labels are not flippable).
K	Set of attacker-controlled data points (labels can be flipped).
K_H	Honest version of K before any label flips.
$D_H = H \cup K_H$	Entire <i>honest</i> training dataset (unmodified).
$D = H \cup K$	Entire training dataset after poisoning (some labels in K may be flipped).
$N = D = D_H $	Total number of data points.
$k = \frac{ K }{ D }$	Fraction of the dataset controlled by the attacker (write-access).
$P \subseteq K$	Subset of K whose labels are actually flipped by the attacker.
b	<i>Local flipping budget</i> (proportion of K that can be label-flipped).
$\mathbb{1}[\cdot]$	Indicator function (returns 1 if the condition is true, 0 otherwise).
$\sigma(\cdot)$	Sigmoid function: $\sigma(z) = \frac{1}{1+e^{-z}}$.
$k \times b$	Corrupted fraction (Global budget)

The main notation used in this work is summarized in Table 1.

Although D and α vary with t (iteration dependent), we omit the epoch index whenever there is no risk of ambiguity since **we treat the attacker’s problem epoch-wise**. By definition $|P| \leq b|K|$. In addition, we use $i \in D$ and $(x_i, y_i) \in D$ interchangeably, and writing $y_i \in K$ means $\{y_i \text{ such that } (x_i, y_i) \in K\}$.

2.2 THREAT MODEL

Rationale. As noted in Bouaziz et al. (2024), the fundamental difference between gradient attacks and data poisoning comes from the limited expressivity of the latter. This difference is even more pronounced for label-flipping. Following the two most relevant works to ours Farhadkhani et al. (2022); Bouaziz et al. (2024), to compare label-flipping and gradient attacks on similar grounds, we consider a threat model in which both attacks can be executed by allowing an attacker to recalculate its attack at each iteration, similarly to Algorithm 1 in Steinhardt et al. (2017).

Setup. We study supervised classification, where each example (x_n, y_n) contains a feature vector $x_n \in \mathbb{R}^{d+1}$ and a label y_n . Suppose that at every training epoch t , a number of workers receive data from a trusted data source and collectively transmit a batch of N examples to the parameter server after processing it. A malicious worker—whom we call *the attacker*—is hidden among them and thus contributes to the final batch with a fixed fraction k of data points, giving the adversary *write access* to that proportion k of the data. It is therefore equivalent to having a malicious worker that contributes a portion k of the final batch. Let K_H denote the clean examples received by the compromised worker. Before forwarding them, the attacker flips the labels of at most a fraction b of these examples—its *local budget*—creating the manipulated set K . The server then trains on $K \cup H$, where $H = \cup_j I_j$ is the unaltered data from the remaining (honest) workers (each contributing I_j). Therefore, no more than a $k \times b$ fraction of the epoch’s batch—the attacker’s *global budget*—is corrupted. Throughout this work, we consider that the server uses *mean aggregation* of gradients.

Figure 3 illustrates this setup. The attacker’s control over data points in K is strictly on their labels; feature vectors remain unaltered. Prior work on gradient-based attacks Bouaziz et al. (2024); Baruch et al. (2019) assumes that the adversary is omniscient, therefore, we allow the attacker to be *omniscient*: they have full *read-access to the model parameters* at every epoch. Further details on the threat model can be found in Appendix C.5.

On the weak adversary Throughout the paper *weaker adversary* refers strictly to the action space: the attacker may only flip labels (under a strict budget, no feature modification, no arbitrary gradient injection). We adopt an omniscient adversary (read access to parameters each round) to align with prevalent threat models in gradient-based poisoning/Byzantine-robust literature Chen et al. (2017); El-Mhamdi et al. (2018); Xie et al. (2018) and to enable a clean comparison: how close can a labels-only attacker get to classical availability attacks? For the more realistic limited-knowledge case, Appendix C.5 shows how an attacker can conceptually train a local surrogate on its accessible subset K_H and apply the same greedy selection there.

2.3 LABEL FLIPPING AS A CONSTRAINED OPTIMIZATION PROBLEM

At epoch t , the server would normally evaluate the empirical loss on the *honest* batch $L_{D_H}(\alpha_t) = \frac{1}{N} \sum_{i \in H \cup K_H} \ell_i(\alpha_t)$, and update the model with the corresponding gradient $\nabla L_{D_H}(\alpha_t)$. However, once the man-in-the-middle adversary flips some labels, the server instead observes the *poisoned* batch $D = H \cup K$ and the loss $L_D(\alpha_t) = \frac{1}{N} \sum_{i \in H \cup K} \ell_i(\alpha_t)$, where ℓ_i is the per-sample cross-entropy loss defined in section 3.

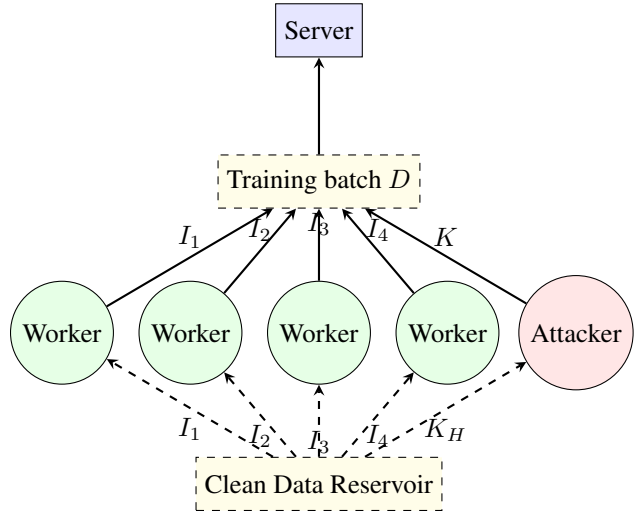


Figure 3: Illustration of the setting: Each user obtains its data from a clean reservoir. The malicious user flips up to a budget b fraction of the labels in K_H .

The attacker decides which labels in K to flip so that the poisoned gradient $\nabla L_D(\alpha_t)$ is as *misaligned* as possible with a chosen direction Δ . We distinguish two goals:

$$\Delta = \begin{cases} -\nabla L_{D_H}(\alpha_t), & \text{untargeted attack,} \\ -(\alpha^{\text{Target}} - \alpha_t), & \text{targeted attack.} \end{cases}$$

The untargeted adversary tries to deviate from the honest gradient, whereas the targeted adversary steers the update toward a pre-selected parameter vector α^{Target} . Figure 4 illustrates how the targeted variant uses the vector $-(\alpha^{\text{Target}} - \alpha_t)$ to bias each gradient step toward α^{Target} . The choice of the target parameter is explained in Appendix A.

Formally, at each epoch t , the attacker solves:

$$\begin{aligned} & \arg \min_{\{y_i^{(D)}\}_{i \in K}} \langle -\nabla L_D(\alpha_t), \Delta \rangle & (1) \\ & \text{s.t. } \underbrace{\sum_{i \in K} \mathbf{1}[y_i^{(D)} \neq y_i^{(D_H)}]}_{\text{(Budget constraint)}} \leq b|K| & \text{(BC)} \end{aligned}$$

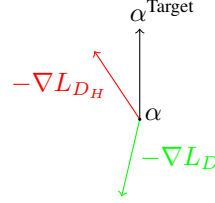


Figure 4: Desired training step direction of honest workers (red), and that of the targeted (black) and untargeted (green) attackers.

where $y_i^{(D_H)}$ are the clean labels received from the compromised worker and $y_i^{(D)}$ are the (possibly flipped) labels that the attacker forwards to the server. The budget constraint (BC) enforces the local budget b : at most a fraction b of the $|K|$ labels under the attacker’s control can be flipped.

3 ATTACK METHOD IN THE BINARY SETTING

In this section, we focus on a binary logistic regression classifier. For a sample $(x_n, y_n) \in \mathbb{R}^{d+1} \times \{0, 1\}$, the *cross-entropy* loss is $l_n(\alpha) = -[y_n \log(\sigma(\alpha^\top x_n)) + (1 - y_n) \log(1 - \sigma(\alpha^\top x_n))]$.

3.1 PROBLEM FORMULATION

At each epoch the server has a parameter vector $\alpha \in \mathbb{R}^{d+1}$ (the last coordinate is the bias) and receives a mini-batch $D = H \cup K$ of size N , where H are honest examples and K are examples under the attacker’s control. For logistic regression, the batch gradient is

$$\nabla L_D(\alpha) = \frac{1}{N} \sum_{n=1}^N (\sigma(\alpha^\top x_n) - y_n) x_n = \frac{|H|}{N} \nabla L_H(\alpha) + \frac{|K|}{N} \nabla L_K(\alpha), \quad (2)$$

with an analogous decomposition for any subset of the data.

Recall from (1) that the adversary chooses the labels in K so as to *anti-align* the poisoned gradient with a reference direction Δ (either the honest gradient or the displacement toward a target model). Because the honest labels are immutable, only the term $\nabla L_K(\alpha)$ matters for the optimization.

Using $\langle \Delta, -\nabla L_K(\alpha) \rangle |K| = \sum_{i \in K} \langle \Delta, x_i \rangle (y_i - \sigma(\alpha^\top x_i))$, the problem (1) simplifies to

$$\arg \min_{\{y_i^{(D)}\}_{i \in K}} \sum_{i \in K} \langle \Delta, x_i \rangle y_i^{(D)} \quad \text{s.t. (BC)}, \quad (3)$$

Where $y_i^{(D)} \in K$ means the label of data point $(x_i, y_i) \in K$.

The objective reveals a clear strategy: to maximise gradient distortion, flip those examples whose feature vectors x_k have the *largest negative* inner product with Δ , i.e. those most misaligned with the desired update direction.

3.2 A GREEDY LABEL-FLIPPING ALGORITHM FOR BINARY CLASSIFICATION

Based on the previous formulation, we now provide an explicit algorithm for the attacker’s label flipping strategy which is *provably optimal at each epoch*. For each attacker-controlled point $(x_i, y_i) \in K$, consider the scalar product $s_i = \langle \Delta, x_i \rangle$. Notice that giving a label of 1 to the points whose s is negative, and a label of 0 to the others will give the minimum of the objective function at the current iteration.

If only a fraction b of the points in K can be flipped, the attacker should focus flips on those x_i that yield the most misaligned values s_i (those that have the greatest magnitude). Concretely, define $p = \lfloor b \cdot |K| \rfloor$. Then: 1. Identify the p points whose s_i is smallest. 2. Flip each of those p points to label 1 if $s_i < 0$, or 0 if $s_i \geq 0$.

If the attacker is allowed to flip *all* data points in K_H , then the strategy is applied to all its points. Algorithm 3 (Appendix A), whose optimality at each epoch is proven in appendix B.1, describes the label flipping strategy. Details on the training algorithm, the hyperparameters, and the target model used can be found in the appendix.

4 BINARY-CLASSIFICATION EXPERIMENTS

4.1 OVERALL ATTACK IMPACT

Experiments on MNIST show that by flipping labels with a global budget $k \times b \leq 25\%$ of the data at each epoch, the attacker can perform an availability attack and keep the model at a random level. Even a global budget of 0.1% reduces the accuracy by around 6%. The exact effect depends on the dataset and model, but the attack tends to be more effective on CIFAR-10, CIFAR-100, and when using an MLP compared to logistic regression.

Another observation is a monotonic trend: increasing k or b strengthens the attacker’s ability to degrade performance or push the parameters toward a desired target. We can also see that for the given b the accuracy decreases as a function of k , however, it is still inherently limited due to the nature of the task and the form of the loss: It is (up to a constant) a linear combination of N feature vectors with binary weights that limits the number of directions we can use during loss minimization.

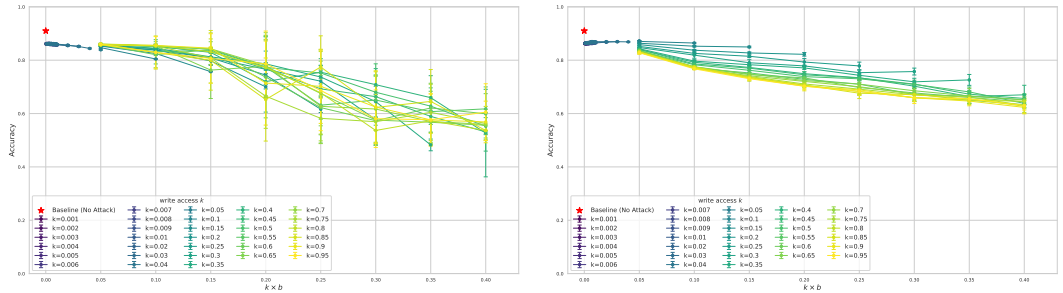


Figure 5: Binary classification: Test accuracy as a function of the global budget under untargeted (left) and targeted (right) attacks, for Mnist (classes 0 and 1).

4.2 UNTARGETED VS TARGETED ATTACKS: IMPACT AND VARIANCE.

The histogram in Figure 6 and the heat map in Figure 7 provide an interesting perspective on how untargeted and targeted label flipping attacks compare in a binary classification setting. At low levels of corruption (for example, $k < 0.1$), both attacks produce a similarly low variance in final accuracy. This indicates that a small amount of label flipping—whether targeted or untargeted—does not drastically affect the stability of model training. However, as k

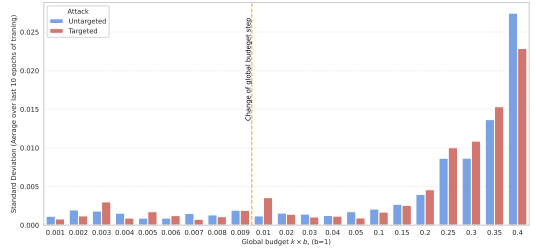


Figure 6: Standard deviation of the final accuracy as a function of k ($b = 1$). The vertical line marks the point where the step size of the x -axis changes.

increases beyond about 0.1, the variance in accuracy begins to grow exponentially, suggesting that the model performance becomes increasingly sensitive to label corruption.

When looking more closely at the interaction between k (write-access) and b (flipping budget), the heatmap in Figure 7 reveals subtle distinctions. Specifically, when $k \lesssim 0.2$, there is very little difference between untargeted and targeted attacks in terms of their overall impact. This similarity makes intuitive sense: at moderate or low corruption rates, flipping is not pervasive enough—whether untargeted or targeted—to cause consistently divergent behaviors in how the model updates its predictions. However, once $k \gtrsim 0.2$, the nature of the attack begins to matter more since untargeted attacks become more efficient, due to the optimality of untargeted attacks.

Nevertheless, the scale of these differences, on the order of 0.2, is not large enough to be of major practical significance in typical real-world use cases. In many binary classification tasks, the difference in mean accuracy (and variance) induced by untargeted versus targeted label flipping is relatively modest. From a robustness standpoint, this suggests that the primary concern should be the overall fraction of corrupted labels rather than the specific pattern of flipping.

4.3 WRITE-ACCESS VS. LOCAL BUDGET TRADE-OFF

Recall that the attacker is omniscient and that they have read-access to all parameters and data of other users, however, they are limited in their write-access by k and by a budget constraint of b . Therefore, given a total flipping proportion $k \times b$, *is it better to increase b and decrease k or vice versa?*

Figure 8 shows the test accuracy for different combinations of k and b . We see that the greater k is, the more effective the attack, and for small k values, b has no impact on the test accuracy. From this, we infer that it is more impactful from the point of view of the attacker to have wide write-access, so the priority is for k before b for a given total flipping proportion $k \times b$. This can be understood by the fact that at each iteration the gradient of the loss as formulated in (2) is a weighted linear combination of the feature vectors, and these weights are linear in the labels which are discrete, which limits the space of gradients to finite set of vectors. Hence, having a greater *write-access* provides a richer space of gradients.

5 EXTENDING THE ATTACK TO MULTI-CLASS TASKS

In this section, we extend our setting to analyze how label flipping affects model performance in the multi-class classification problem. Consider that we have C classes and again N data points and define a matrix \mathbf{T} that encodes the classes of data points in D . We use one hot encoding to encode classes and cross entropy as the loss. For $c \in [1, C]$ and $n \in [1, N]$, \mathbf{T}_{cn} corresponds to whether the n -th data point has label c or not: $\mathbf{T}_{cn} = 1$ if $y^{(n)} = c$ and $\mathbf{T}_{cn} = 0$ otherwise. And let $W \in \mathbb{R}^{C \times (d+1)}$ be the matrix of parameters of the logistic regression model.

The cross entropy loss can be written as:

$$L_D(W) = - \sum_{n=1}^N \sum_{c=1}^C \mathbf{T}_{cn} \log p(\mathbf{T}_{cn} = 1 | \mathbf{x}^{(n)}, W) = - \sum_{n=1}^N \sum_{c=1}^C \mathbf{T}_{cn} \log \text{softmax}(\mathbf{W}\mathbf{x}^{(n)})_c$$

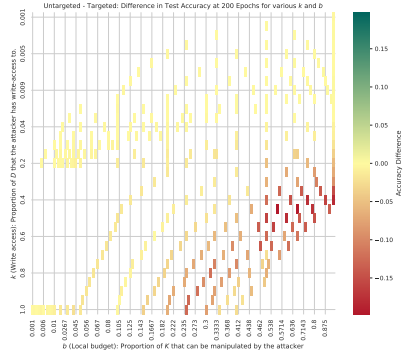


Figure 7: Heatmap of the difference of test accuracies between an untargeted attack and a targeted attack.

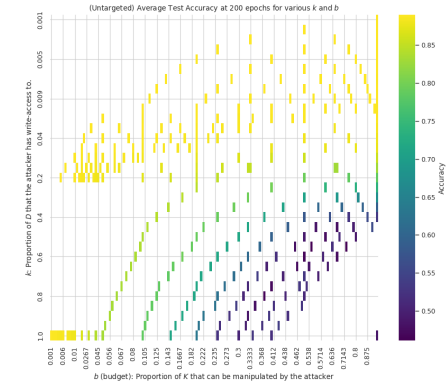


Figure 8: Heatmap of test accuracy as a function of k and b at 200 epochs for the untargeted attack.

Following the same idea as in the binary setting, the attacker wants to flip labels to control the gradient. Let $\nabla_j L_D$ be the gradient of the loss on dataset D with respect to the j^{th} row of W .

$$\begin{aligned}\nabla_j L_D &= \frac{\partial L_D}{\partial W_{j,\bullet}} = - \sum_{n=1}^N \sum_{c=1}^C \mathbf{T}_{cn} \frac{1}{\text{softmax}(\mathbf{W}\mathbf{x}^{(n)})_c} \frac{\partial}{\partial W_{j,\bullet}} \text{softmax}(\mathbf{W}\mathbf{x}^{(n)})_c \\ &= - \sum_{n=1}^N \sum_{c=1}^C \mathbf{T}_{cn} \left(\mathbb{1}[c=j] - \text{softmax}(\mathbf{W}\mathbf{x}^{(n)})_j \right) \mathbf{x}^{(n)}\end{aligned}$$

Where $\mathbb{1}[\cdot]$ is the indicator function.

For $j \in [1, C]$, let $\Delta_j = \begin{cases} -\nabla_j L_{D_H}, & \text{(untargeted attack)} \\ -(W^{\text{Target}} - W_t), & \text{(targeted attack)} \end{cases}$ where W^{Target} is a target model and W_t the model at the iteration t . The optimization problem of the attacker at each epoch is to minimize the Frobenius inner product:

$$\begin{aligned}\arg \min_{T \in \{0,1\}^{C \times N}} & \sum_{j=1}^C F_j(T) \\ \text{s.t.} & \begin{cases} F_j = \langle \nabla_j L_D, -\Delta_j \rangle = \sum_{n=1}^N \sum_{c=1}^C T_{cn} \left(\mathbb{1}_{\{c=j\}} - \text{softmax}(W x^{(n)})_j \right) \langle x^{(n)}, \Delta_j \rangle, \\ \sum_{c=1}^C T_{cn} = 1 \quad (\forall n), \\ \text{(BC)} \end{cases}\end{aligned}$$

Let $Z_{cn} = \sum_{j=1}^C \langle x^{(n)}, \left(\mathbb{1}[c=j] - \text{softmax}(\mathbf{W}\mathbf{x}^{(n)})_j \right) \Delta_j \rangle$. The constraints impose that $\sum_{c=1}^C \mathbf{T}_{cn} Z_{cn}$ is in reality just one term. Therefore, for $n \in K$, take $c^{(n^*)}$ as the index of the minimum of $(Z_{cn})_{c \in C}$ and assign $T_{cn} = 1$ if $c = c^{(n^*)}$ and 0 otherwise, starting with the Z_{cn} s that yield the least until we run out of budget. Taking such labels that minimize Z_{cn} for every n ensures that the attacked gradient is minimal across all other possible label choices. Meaning that the algorithm is per-epoch optimal. Algorithm 1 details the procedure.

Algorithm 1 Per-epoch greedy label selection (multi-class)

Require: Attacker set $K = \{x^{(n)}\}_{n \in K}$, current weight matrix $W_t \in \mathbb{R}^{C \times (d+1)}$, vectors Δ_j for $j = 1, \dots, C$, local budget fraction $b \in (0, 1]$

Ensure: Label assignment indicators $T \in \{0, 1\}^{C \times N}$ for $n \in K$

- 1: $p \leftarrow \lfloor b \cdot |K| \rfloor$
- 2: **for** each $n \in K$ **do**
- 3: **for** each class $c \in \{1, \dots, C\}$ **do**
- 4: compute

$$Z_{cn} \leftarrow \sum_{j=1}^C \langle x^{(n)}, (\mathbb{1}[c=j] - \text{softmax}(W_t x^{(n)})_j) \Delta_j \rangle$$

- 5: **end for**
 - 6: $c^*(n) \leftarrow \arg \min_c Z_{cn}$
 - 7: $Z_{\min}(n) \leftarrow Z_{c^*(n),n}$
 - 8: **end for**
 - 9: Sort indices $n \in K$ by ascending $Z_{\min}(n)$ and select the p smallest indices S .
 - 10: **for** each $n \in S$ **do**
 - 11: Set $T_{c^*(n),n} \leftarrow 1$ and $T_{c,n} \leftarrow 0$ for $c \neq c^*(n)$
 - 12: **end for**
 - 13: **Return** T
-

6 MULTI-CLASS EXPERIMENTAL RESULTS

Experimental setup. All experiments report means \pm standard variation over 6 independent runs. Datasets: MNIST, CIFAR-10, CIFAR-100 (details in App. A). Models: logistic regression (main) and a 2-layer MLP. Data splits are iid across workers. Optimizers: SGD (main) and Adam (ablation, App. A). Metrics: test accuracy and F1-score. All the figures are shown for Mnist dataset (where the attack has the least impact across the datasets tested). Results for the other datasets and the vanilla neural network is in Appendix D.

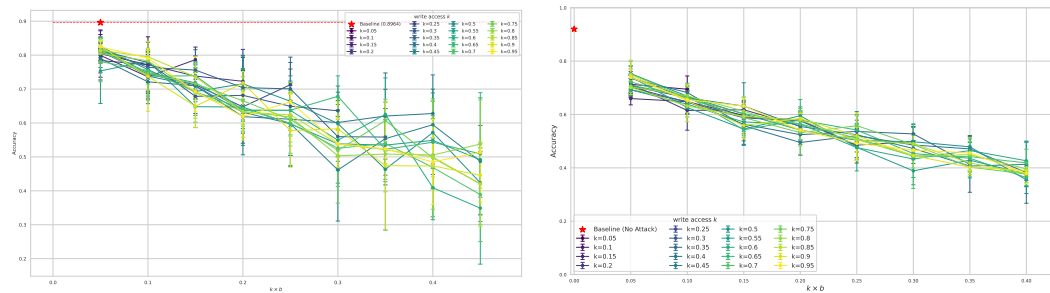


Figure 9: Test accuracy vs. global budget under untargeted (left) and targeted (right) attacks, for Mnist10 dataset (unnormalized).

Figure 9 shows the attack results. Each plotted point reports the average test accuracy as a function of the fraction of modified points, and is an average over 6 runs. It shows that for just a global budget of 5% of the dataset, the attacks dropped the test accuracy by 10 – 19%. Moreover, Figure 10 shows that the variance of an untargeted attack is greater than that of a targeted attack, confirming the idea that untargeted attacks are more chaotic since they are not directed whereas targeted attacks are more guided and hence less erratic. Also, comparing Figure 10 with Figure 6 shows that the magnitude of the accuracy’s variance under attack grows with the number of classes, going from around 0.02 to 0.1 as the number of classes goes from 2 to 10. Which suggests that effect of the proposed attack on the accuracy’s variance grows with the number of classes.

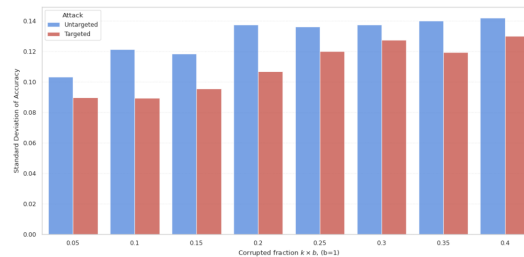


Figure 10: Standard deviation of test accuracy vs global budget (b fixed =1) for the multi-class classification setting.

Detectability and data normalization. Many practical FL pipelines normalize or scale features prior to training. We empirically observe that under min-max normalization the attacker’s per-client gradient norm is nearly indistinguishable from honest clients (see Table 3 in Appendix F). Consequently, defenses that clip updates based solely on gradient norm thresholds are ineffective in normalized settings. When inputs are unnormalized, the gradient-norm disparity becomes large and simple norm-based defenses regain efficacy. That’s a limitation of the attacker since he can’t control the features.

7 CONCLUSION

In this study, we demonstrate that a purely *label-flipping* adversary - constrained by a strict budget and guided only by a greedy rule - can launch an availability attack. By introducing an intuitive, budget-aware objective, we reveal a vulnerability previously believed to require gradient overwrites or feature-level poisoning. Both targeted and untargeted flips destabilize training and reduce test accuracy. Our experiments on several benchmarks confirm the potency of the attack relative to the state-of-the-art baselines. These findings establish a foundation for stronger defenses and, more broadly, a deeper understanding of security in federated and distributed learning. Interesting follow-up avenues could include (i) generalizing the attack to deep networks and non-mean aggregators (e.g.

486 medians); (ii) searching for globally optimal flipping attacks; and (iii) devising practical defenses
487 tailored to the proposed threat model. We believe that our work establishes a solid foundation for
488 future advancements in secure and robust federated learning.

490 REFERENCES

- 491
492 Pranjali Awasthi, Maria Florina Balcan, and Philip M. Long. The power of localization for efficiently
493 learning linear separators with noise. 63(6), 2017. ISSN 0004-5411. doi: 10.1145/3006384. URL
494 <https://doi.org/10.1145/3006384>.
- 495
496 Melis Ilayda Bal, Volkan Cevher, and Michael Muehlebach. Adversarial training for de-
497 fense against label poisoning attacks. In Y. Yue, A. Garg, N. Peng, F. Sha, and R. Yu
498 (eds.), *International Conference on Representation Learning*, volume 2025, pp. 16235–16269,
499 2025. URL [https://proceedings.iclr.cc/paper_files/paper/2025/file/
500 298c3e32d7d402189444be2ff5d19979-Paper-Conference.pdf](https://proceedings.iclr.cc/paper_files/paper/2025/file/298c3e32d7d402189444be2ff5d19979-Paper-Conference.pdf).
- 501
502 Gilad Baruch, Moran Baruch, and Yoav Goldberg. A little is enough: Circumventing defenses for
503 distributed learning. *Advances in Neural Information Processing Systems*, 2019.
- 504
505 Peva Blanchard, El Mahdi El Mhamdi, Rachid Guerraoui, and Julien Stainer. Machine learning
506 with adversaries: Byzantine tolerant gradient descent. *Advances in neural information processing
507 systems*, 30, 2017.
- 508
509 Wassim Bouaziz, El-Mahdi El-Mhamdi, and Nicolas Usunier. Inverting gradient attacks makes
510 powerful data poisoning. *arxiv:2410.21453*, 2024.
- 511
512 Yudong Chen, Lili Su, and Jiaming Xu. Distributed statistical machine learning in adversarial settings:
513 Byzantine gradient descent. *Proceedings of the ACM on Measurement and Analysis of Computing
514 Systems*, 1(2):1–25, 2017.
- 515
516 El-Mahdi El-Mhamdi, Rachid Guerraoui, and Sébastien Rouault. The hidden vulnerability of
517 distributed learning in byzantium. *International Conference on Machine Learning*, 2018.
- 518
519 Sadeq Farhadkhani, Lê-Nguyên Hoang, and Oscar Villemaud. An equivalence between data
520 poisoning and byzantine gradient attacks. In *International Conference on Machine Learning*, 2022.
- 521
522 Jonas Geiping, Liam Fowl, W Ronny Huang, Wojciech Czaja, Gavin Taylor, Michael Moeller, and
523 Tom Goldstein. Witches’ brew: Industrial scale data poisoning via gradient matching. *arXiv
524 preprint arXiv:2009.02276*, 2020.
- 525
526 Ling Huang, Anthony D. Joseph, Blaine Nelson, Benjamin I.P. Rubinstein, and J. D. Tygar. Ad-
527 versarial machine learning. In *Proceedings of the 4th ACM Workshop on Security and Arti-
528 ficial Intelligence, AISec ’11*, pp. 43–58, New York, NY, USA, 2011. Association for Com-
529 puting Machinery. ISBN 9781450310031. doi: 10.1145/2046684.2046692. URL [https:
530 //doi.org/10.1145/2046684.2046692](https://doi.org/10.1145/2046684.2046692).
- 531
532 W Ronny Huang, Jonas Geiping, Liam Fowl, Gavin Taylor, and Tom Goldstein. Metapoison: Practical
533 general-purpose clean-label data poisoning. *Advances in Neural Information Processing Systems*,
534 2020.
- 535
536 Rishi D. Jha, Jonathan Hayase, and Sewoong Oh. Label poisoning is all you need. In *Proceedings
537 of the 37th International Conference on Neural Information Processing Systems, NIPS ’23*, Red
538 Hook, NY, USA, 2023. Curran Associates Inc.
- 539
540 Sai Praneeth Karimireddy, Lie He, and Martin Jaggi. Byzantine-robust learning on heterogeneous
541 datasets via bucketing. In *International Conference on Learning Representations*, 2020. URL
542 <https://api.semanticscholar.org/CorpusID:238856649>.
- 543
544 Pang Wei Koh, Jacob Steinhardt, and Percy Liang. Stronger data poisoning attacks break data
545 sanitization defenses. *Machine Learning*, pp. 1–47, 2022.

- 540 Léo Lavour, Yann Busnel, and Fabien Autrel. Systematic analysis of label-flipping attacks against
541 federated learning in collaborative intrusion detection systems. In *Proceedings of the 19th International
542 Conference on Availability, Reliability and Security, ARES '24*, New York, NY, USA, 2024.
543 Association for Computing Machinery. ISBN 9798400717185. doi: 10.1145/3664476.3670434.
544 URL <https://doi.org/10.1145/3664476.3670434>.
- 545 Yann LeCun, Corinna Cortes, and CJ Burges. Mnist handwritten digit database. *ATT Labs [Online].
546 Available: <http://yann.lecun.com/exdb/mnist>*, 2, 2010.
547
- 548 Qingru Li, Xinru Wang, Fangwei Wang, and Changguang Wang. A label flipping attack on ma-
549 chine learning model and its defense mechanism. In *Algorithms and Architectures for Parallel
550 Processing: 22nd International Conference, ICA3PP 2022, Copenhagen, Denmark, October
551 10–12, 2022, Proceedings*, pp. 490–506, Berlin, Heidelberg, 2022. Springer-Verlag. ISBN 978-
552 3-031-22676-2. doi: 10.1007/978-3-031-22677-9_26. URL [https://doi.org/10.1007/
553 978-3-031-22677-9_26](https://doi.org/10.1007/978-3-031-22677-9_26).
- 554 Yiyong Liu, Michael Backes, and Xiao Zhang. Transferable availability poisoning attacks.
555 *arXiv:2310.05141*, 2023a.
556
- 557 Yuchen Liu, Chen Chen, Lingjuan Lyu, Fangzhao Wu, Sai Wu, and Gang Chen. Byzantine-robust
558 learning on heterogeneous data via gradient splitting. In *Proceedings of the 40th International
559 Conference on Machine Learning, ICML'23*. JMLR.org, 2023b.
- 560 Yiwei Lu, Gautam Kamath, and Yaoliang Yu. Indiscriminate data poisoning attacks on neural
561 networks. *ArXiv*, abs/2204.09092, 2022. URL [https://api.semanticscholar.org/
562 CorpusID:248266720](https://api.semanticscholar.org/CorpusID:248266720).
- 563 Brendan McMahan, Eider Moore, Daniel Ramage, Seth Hampson, and Blaise Agüera y Arcas.
564 Communication-efficient learning of deep networks from decentralized data. In Aarti Singh
565 and Xiaojin (Jerry) Zhu (eds.), *Proceedings of the 20th International Conference on Artificial
566 Intelligence and Statistics, AISTATS 2017, 20-22 April 2017, Fort Lauderdale, FL, USA*, volume 54
567 of *Proceedings of Machine Learning Research*, pp. 1273–1282. PMLR, 2017. URL [http:
568 //proceedings.mlr.press/v54/mcmahan17a.html](http://proceedings.mlr.press/v54/mcmahan17a.html).
- 569
- 570 Rui Ning, Jiang Li, Chunsheng Xin, and Hongyi Wu. Invisible poison: A blackbox clean label
571 backdoor attack to deep neural networks. In *IEEE INFOCOM 2021-IEEE Conference on Computer
572 Communications*, pp. 1–10. IEEE, 2021.
- 573
- 574 Andrea Paudice, Luis Muñoz-González, and Emil C. Lupu. Label sanitization against label flipping
575 poisoning attacks, 2018. URL <https://arxiv.org/abs/1803.00992>.
- 576
- 577 Jie Peng, Weiyu Li, Stefan Vlaski, and Qing Ling. Mean aggregator is more robust than robust
578 aggregators under label poisoning attacks on distributed heterogeneous data. *Journal of Machine
579 Learning Research*, 26(27):1–51, 2025. URL [http://jmlr.org/papers/v26/24-1307.
580 html](http://jmlr.org/papers/v26/24-1307.html).
- 581
- 581 Ali Shafahi, W. Ronny Huang, Mahyar Najibi, Octavian Suci, Christoph Studer, Tudor Dumitras,
582 and Tom Goldstein. Poison frogs! targeted clean-label poisoning attacks on neural networks, 2018.
583 URL <https://arxiv.org/abs/1804.00792>.
- 584
- 584 Virat Shejwalkar, Amir Houmansadr, Peter Kairouz, and Daniel Ramage. Back to the drawing board:
585 A critical evaluation of poisoning attacks on federated learning. *CoRR*, abs/2108.10241, 2021.
586 URL <https://arxiv.org/abs/2108.10241>.
- 587
- 588 Jacob Steinhardt, Pang Wei W Koh, and Percy S Liang. Certified defenses for data poisoning attacks.
589 *Advances in neural information processing systems*, 30, 2017.
- 590
- 590 Ziteng Sun, Peter Kairouz, Ananda Theertha Suresh, and H. Brendan McMahan. Can you really
591 backdoor federated learning?, 2019. URL <https://arxiv.org/abs/1911.07963>.
- 592
- 593 Cong Xie, Oluwasanmi Koyejo, and Indranil Gupta. Generalized byzantine-tolerant SGD. *CoRR*,
abs/1802.10116, 2018. URL <http://arxiv.org/abs/1802.10116>.

594 Shanqing Yu, Jie Shen, Shaocong Xu, Jinhuan Wang, Zeyu Wang, and Qi Xuan. Label-flipping
 595 attacks in gnn-based federated learning. *IEEE Transactions on Network Science and Engineering*,
 596 12(2):1357–1368, 2025. doi: 10.1109/TNSE.2025.3528831.

597
 598 Chiyuan Zhang, Samy Bengio, Moritz Hardt, Benjamin Recht, and Oriol Vinyals. Understanding
 599 deep learning requires rethinking generalization, 2017. URL [https://arxiv.org/abs/](https://arxiv.org/abs/1611.03530)
 600 1611.03530.

601
 602 Bingyin Zhao and Yingjie Lao. CLPA: Clean-Label Poisoning Availability Attacks Using Generative
 603 Adversarial Nets. In *Proceedings of the AAAI Conference on Artificial Intelligence*, volume 36, pp.
 604 9162–9170, 2022. doi: 10.1609/aaai.v36i8.20902. URL [https://ojs.aaai.org/index.](https://ojs.aaai.org/index.php/AAAI/article/view/20902)
 605 [php/AAAI/article/view/20902](https://ojs.aaai.org/index.php/AAAI/article/view/20902).

606 607 608 APPENDIX

609
 610 This appendix is organised as follows, section A details the datasets, data splits, target models, and
 611 training protocol, and provides the end-to-end pseudocode used in our experiments. In Section E,
 612 we examine robustness under alternative metrics and optimizers: the F1 score and test accuracy
 613 degrade monotonically with the corrupted fraction $k \times b$, early stopping amplifies this effect, and
 614 Adam exhibits larger drops than SGD. Section B.1 presents the proof that our label-selection rule is
 615 greedy-optimal at each epoch. We then justify the focus on mean aggregation, arguing it remains
 616 a strong and practically relevant baseline and that our labels-only attack operates within valid
 617 gradient magnitudes, limiting the effectiveness of norm-based defenses. Subsequent sections discuss
 618 data distribution assumptions—our attack is distribution-agnostic and heterogeneity can further
 619 hinder robust aggregators—and clarify the threat model: we analyze an omniscient adversary for
 620 comparability and outline how a surrogate-based attacker can operate with partial knowledge.

621 A DATASET AND EXPERIMENTAL SETUP

622
 623 **Dataset.** We perform all experiments on the MNIST (LeCun et al. (2010)) handwritten-digit
 624 corpus, CIFAR-10 and CIFAR-100. Each image was flattened for the logistic regression model
 625 and we maintained the original pixel intensity scale without additional normalization for the main
 626 experiments. We later discuss the effect of normalization in Appendix F.

Name	# Features	# Train/test	Target model
MNIST (0 vs 1)	28×28	6903 / 7877	Fully flipped ($0 \leftrightarrow 1$)
CIFAR10 (airplane vs automobile)	$3 \times 32 \times 32$	5000 / 1000	Fully flipped (airplane \leftrightarrow automobile)
MNIST (10-class)	28×28	60000 / 10000	Cyclic shift $y \mapsto (y + 1) \bmod 10$
CIFAR10 (10-class)	$3 \times 32 \times 32$	50000 / 10000	Cyclic shift $y \mapsto (y + 1) \bmod 10$
CIFAR100 (100-class)	$3 \times 32 \times 32$	50000 / 10000	Cyclic shift $y \mapsto (y + 1) \bmod 100$

627
628
629
630
631
632
633
634
635
636
637 Table 2: Datasets and target models.

638
 639 **Choice of target parameter vector.** For the targeted label-flip attack we adopt a deterministic rule
 640 for selecting the adversarial target label. Specifically, we use a cyclic permutation of class indices:
 641 for any original label $y_i \in \{0, \dots, 9\}$, the attacker sets
 642

$$643 \quad y'_i \leftarrow (y_i + 1) \bmod 10.$$

644
 645 To obtain the target parameter vector/matrix $\alpha^{\text{Target}}/W^{\text{Target}}$ used in the optimization, we train an
 646 honest model on the previously *flipped* dataset. The final parameters of that trained model constitute
 647 $\alpha^{\text{Target}}/W^{\text{Target}}$; the attacker then attempts to steer the server model toward these parameters via the
 targeted attack.

Implementation Details. We train logistic regression classifiers for 200 epochs using mini-batch SGD with a batch size of 64 and a learning rate of 0.001, using cross-entropy loss. At each epoch, the omniscient attacker observes the current model parameters and gradients, then flips the labels of a randomly assigned subset K from the clean data pool accordingly. All results are averaged over six independent runs with different random seeds. The global training algorithm can be found below (Algorithm 2).

Algorithm 2 Full Training with Label Flipping Attack

Require: Clean dataset D , model M , total epochs E , budgets k and b , and functions:

- `getSubset`: retrieves the attacker’s subset randomly from D , of size $k \times |D|$.
- `selectFlip`: determines which labels to flip, and flips accordingly using Algorithms 3 and 1.
- `trainStep`: performs one training iteration.

Ensure: Poison-trained model M

```

1: Initialize model  $M$ 
2: for epoch  $\leftarrow 1$  to  $E$  do
3:    $K_H \leftarrow \text{getSubset}(D, k)$ 
4:    $K \leftarrow \text{selectFlip}(D, K, M, b)$ 
5:    $M \leftarrow \text{trainStep}(M, (D \setminus K_H) \cup K)$  {Train on poisoned dataset}
6:    $D \leftarrow (D \setminus K) \cup K_H$  {Clean D for next iterations}
7: end for
8: return  $M$ 

```

The greedy label flipping attack in the binary setting We present Algorithm 3, the greedy label flipping attack algorithm used for binary classification.

Algorithm 3 The greedy label flipping attack for binary classification.

Require: Attacker set $K = \{(x_i, y_i)\}$; budget $b \in (0, 1)$; honest gradient $\nabla L_{D_H}(\alpha)$ at current epoch t .

$p \leftarrow \lfloor b \cdot |K| \rfloor$.

$$\Delta \leftarrow \begin{cases} -\nabla L_{D_H}(\alpha), & \text{(untargeted attack)} \\ -(\alpha^{\text{Target}} - \alpha_t), & \text{(targeted attack)} \end{cases}$$

for each $i \in K$ **do**

$s_i \leftarrow \langle \Delta, x_i \rangle$.

end for

Find the p indices i with the smallest s_i .

for each selected index i **do**

if $s_i < 0$ **then**

$y_i \leftarrow 1$.

else

$y_i \leftarrow 0$.

end if

end for

B ON THE GREEDINESS OF THE PROPOSED ALGORITHMS

B.1 PROOF OF THE GREEDINESS

We now show that Algorithm 3 label flips *provably minimize* the attacker’s objective *at each epoch*.

First, recall the following lemma:

Lemma B.1 (Rearrangement Inequality). *For any real numbers $x_1 \leq x_2 \leq \dots \leq x_n$ and $y_1 \leq y_2 \leq \dots \leq y_n$, and for every permutation σ of $\{1, 2, \dots, n\}$,*

$$x_1 y_n + x_2 y_{n-1} + \dots + x_n y_1 \leq \sum_{i=1}^n x_i y_{\sigma(i)} \leq x_1 y_1 + x_2 y_2 + \dots + x_n y_n.$$

Proof. Recall that for each attacker-controlled point $i \in K$, we define

$$s_i = \langle \Delta, x_i \rangle, \quad \text{where } \Delta = -\nabla L_{D_H}(\alpha).$$

The attacker’s task is to solve

$$\min_{\{y_i\}_{i \in K}} \sum_{i \in K} s_i y_i \quad \text{subject to} \quad \sum_{i \in K} \mathbb{1}[y_i^{(D)} \neq y_i^{(D_H)}] \leq b |K|,$$

where $y_i \in \{0, 1\}$ are the (possibly flipped) labels under budget b .

Let $m = |K|$, and assume $s_{(1)} \leq s_{(2)} \leq \dots \leq s_{(m)}$ is the ascending order of the scalar products. Then we can re-index the labels as $\mathbf{y} = (y_{(1)}, y_{(2)}, \dots, y_{(m)})$ so that $y_{(j)}$ pairs with $s_{(j)}$.

By the Rearrangement Inequality (Lemma B.1), for two sorted sequences $\{x_1 \leq \dots \leq x_m\}$ and $\{y_1 \leq \dots \leq y_m\}$, the minimum of $\sum_{j=1}^m x_j y_{\sigma(j)}$ over all permutations σ occurs when the largest x_j pairs with the smallest y_j , and vice versa. In our case, $y_i \in \{0, 1\}$. Thus, to minimize $\sum_{i \in K} s_i y_i$, we should assign $y_i = 1$ to the smallest s_i (those that are negative) and $y_i = 0$ to the largest s_i (nonnegative)—exactly as in Algorithm 3. Constrained by $\lfloor b |K| \rfloor$ total flips, the attacker picks the $\lfloor b |K| \rfloor$ smallest s_i to flip to 1 when $s_i < 0$, or to 0 if $s_i \geq 0$. This guarantees local optimality at each epoch.

B.2 ON THE OPTIMALITY OF THE APPROACH

While Lemma B.1 proves that our greedy label-selection rule is optimal within a single training epoch, this guarantee does not extend automatically to the full training trajectory. Temporal coupling of successive updates can in principle produce cancellations: a flip that maximally misaligns the gradient at step t might later be undone by the dynamics of the optimizer or by subsequent updates. Constructing a globally optimal sequence of flips therefore requires solving a combinatorial, horizon-wide optimization problem (or equivalently optimizing over label sequences), which would be computationally intractable in realistic settings and would impose substantial computational overhead compared to our per-epoch rule. Therefore, conceptually, non-greedy strategies could sometimes outperform the per-epoch greedy policy, but any practical implementation must trade off attack effectiveness against the high computational requirements of such methods.

Also, even if an individual poisoned gradient is later partially reversed, that intermediate misdirection still disrupts the optimizer’s path and can significantly slow convergence – a cost that translates directly into extra training iterations (and thus compute and monetary cost) for large models.

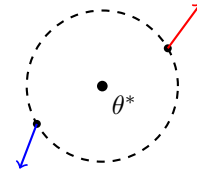


Figure 11: Illustration of temporal oscillation: two successive poisoned gradients can point in approximately opposite directions relative to the θ^* . Even when later updates partially cancel earlier misdirections, the transient deviations still perturb the optimizer’s trajectory and can increase training cost or degrade final performance.

C DISCUSSION

C.1 HOW PRACTICAL IS THE ATTACK?

In addition to our formal threat model, we note several realistic settings where label-only corruption can occur in production systems:

- 756 • Compromised labeling tools: attackers who can modify annotation UIs, metadata, or labeling
757 scripts can change labels stored in databases while leaving raw sensor data untouched.
- 758
- 759 • Insider at a data provider: an employee with access to label fields (but not feature pipelines)
760 can flip labels locally.
- 761
- 762 • Crowdsourced annotation manipulation: attackers controlling a subset of crowd workers or
763 poisoning weakly-supervised labeling heuristics can flip a small fraction of labels across
764 contributors.

765 C.2 WHY LOGISTIC REGRESSION

766

767 There are two reasons why we adopt logistic regression as a first-class test bed: (i) *Analytic trans-*
768 *parency*. The loss is convex and its gradient admits a simple closed form, allowing us to derive our
769 greedy attacks. (ii) *Gateway to richer models*. Any classifier whose final layer is linear followed
770 by a sigmoid/softmax (e.g. multilayer networks, convolutional nets) reduces to logistic regression
771 if we treat the penultimate activations as “features.” Consequently, at each training step our attack
772 should apply to those models by operating on the last-layer logits.¹ This raises the question: Would
773 such an attack still be greedy for any classifier? One path to performing a label-flipping attack on
774 a broader class of models could be the transition from logistic regression to neural networks. We
775 perform preliminary experiments on a 2-layer vanilla MLP using the method described above, the
776 results can be found in Appendix D. Another approach is to find a globally optimal label flipping
777 attack algorithm. We assumed that the server was aggregating the gradients using the mean, and a
778 future work would discuss similar attacks on settings with different aggregation methods presented in
779 Baruch et al. (2019); El-Mhamdi et al. (2018); Blanchard et al. (2017).

780 C.3 WHY MEAN AGGREGATION STILL MATTERS

781

782 Our focus on mean aggregation is intentional: it establishes a baseline benchmark for the impact of
783 label-flipping attacks. If such an attack fails here, it is unlikely to succeed against more sophisticated
784 robust aggregators; if it succeeds, it provides a clear lower bound that any robust method should
785 surpass. Moreover, our attack design is specifically derived for the mean operator, and different
786 aggregation rules would require different attack formulations. In real-world deployments, where
787 FedAvg is still prevalent, understanding vulnerabilities under mean aggregation is crucial for designing
788 defenses.

789 Further, our results are meant as an opening for constrained label flipping attacks. By demonstrating
790 that the constrained label-flipping attack is feasible against the most common aggregation rule, we
791 establish the case for extending our methodology to robust aggregation methods as a natural next
792 step. We also note that some defenses like norm clipping (which are shown very efficient in practice
793 in combination with mean aggregation (Sun et al. (2019))) are inherently blind against our approach,
794 since the attack operates in the space of valid gradient updates derived from valid gradient vectors
795 generated by plausible label flips, where feature inputs are untouched. Since every flipped label still
796 produces a legitimate gradient, clipping based solely on gradient norm is unable to distinguish or
797 suppress malicious updates that conform to honest-looking magnitudes-making our attack inherently
798 robust against such defenses. This further values studying mean aggregation as a baseline before
799 moving to more complex settings.

800 C.4 ON THE DATA DISTRIBUTION

801

802 Our experiments used a uniform i.i.d. data split across workers. All clients sampled from the same
803 distribution and contributed equal-sized batches. However, our attack is distribution-agnostic: it does
804 not assume i.i.d. data and optimizes flips online per iteration. In fact, heterogeneity generally makes
805 many robust aggregation rules less reliable; non-IID gradients enlarge natural variability, which both
806 weakens anomaly tests and can cause robust rules (e.g., trimming) to underperform FedAvg in certain
807 regimes (Liu et al. (2023b)).

808

809 ¹Formally, let $f_\theta(X) = \sigma(W h_\phi(X))$ with inner network h_ϕ fixed during one optimization step. Setting
 $\tilde{X} = h_\phi(X)$ recasts the update as a logistic regression in (\tilde{X}, y) with parameter W .

As attacks are easier in heterogeneous settings, and harder in homogeneous ones (Peng et al. (2025); Karimireddy et al. (2020)), our work highlights the power of label flipping even on i.i.d. (and thus less vulnerable) situations.

C.5 ON THE THREAT MODEL

What if the attacker lacks omniscience In the case where the attacker lacks full knowledge, for example consider a scenario where the attacker knows the architecture of the server’s model but not its current parameters. Then the attacker can train a local surrogate model using only the data available to them (i.e., the subset they control). This local model may not perfectly match the server’s model, but it can still approximate the decision boundary or the gradient dynamics well enough to inform a useful attack.

Specifically, the attacker can simulate the label-flipping attack on their local model concurrently with the server’s training. By observing how different label flips affect the gradient direction or training loss on their surrogate, the attacker can estimate which flips are most likely to have the desired effect when sent to the server. This strategy may reduce the attack’s effectiveness but remain viable.

D EXPERIMENTS ON MORE DATASETS AND EXTENSION TO DEEP MODELS

Across MNIST10, CIFAR10, and CIFAR100, for both logistic regression and a 2-layer MLP, we observe a consistent pattern: our greedy label-flipping attack remains effective even when the model becomes deeper or the dataset becomes more complex or there are more classes.

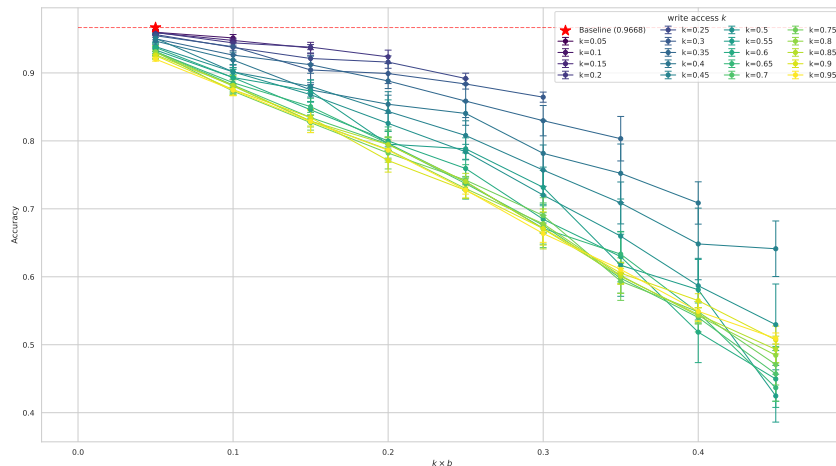


Figure 12: 2-layer vanilla MLP model on MNIST10 dataset

The curves for different write-access values k remain well separated, confirming the same trend seen in the logistic regression experiments: write-access is more important than the local flipping budget. The MNIST10 task is relatively easy, and the MLP achieves a high baseline accuracy. Yet even here, modest flipping budgets already produce visible degradation.

In contrast to MNIST10, results on CIFAR10 are noisier and the magnitude of degradation is smaller. Logistic regression is a weak model for CIFAR10, and the baseline accuracy is close to random guessing. As a result, the attack has limited room to reduce performance further, and much of the observed variance comes from the underlying difficulty of the task (maybe related to the signal to noise ratio of the data) rather than the attack.

Moving from logistic regression to a 2-layer MLP increases representational capacity, and the attack again becomes effective. While the curves remain relatively noisy, the overall trend is that high k settings usually incur the most damage. This demonstrates that the greedy rule generalizes reasonably well to non-convex models, even though we do not claim theoretical optimality beyond logistic regression.

864
865
866
867
868
869
870
871
872
873
874
875
876
877
878
879
880
881
882
883
884
885
886
887
888
889
890
891
892
893
894
895
896
897
898
899
900
901
902
903
904
905
906
907
908
909
910
911
912
913
914
915
916
917

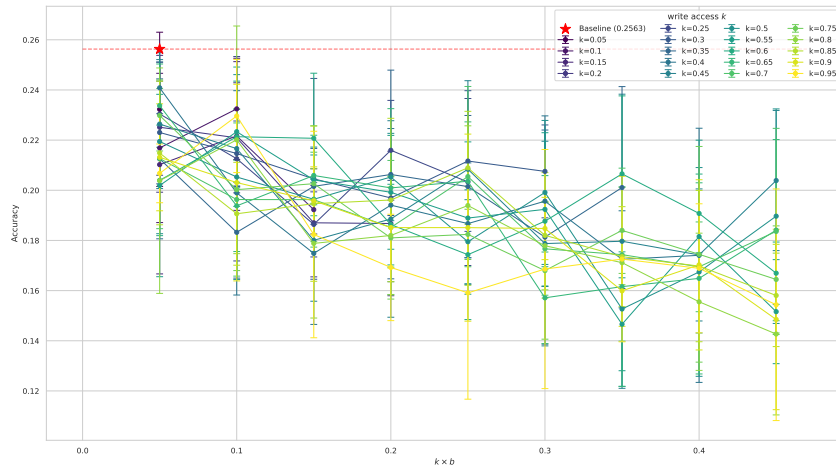


Figure 13: Logistic regression model on CIFAR10 dataset

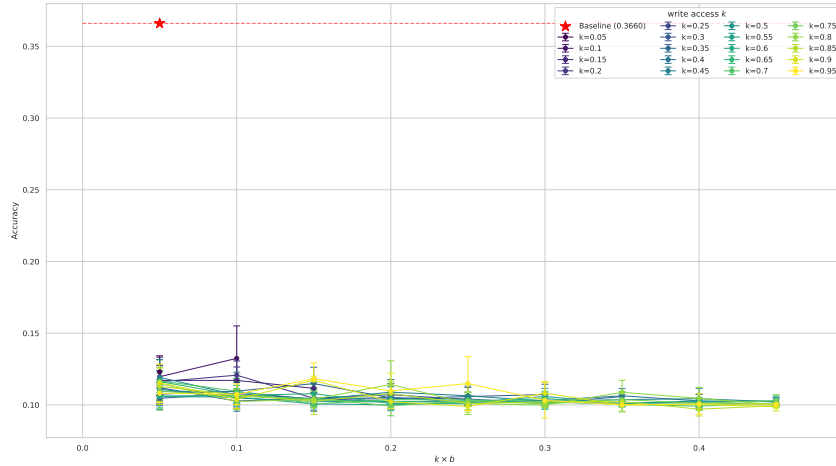


Figure 14: 2-layer vanilla MLP model on CIFAR10 dataset

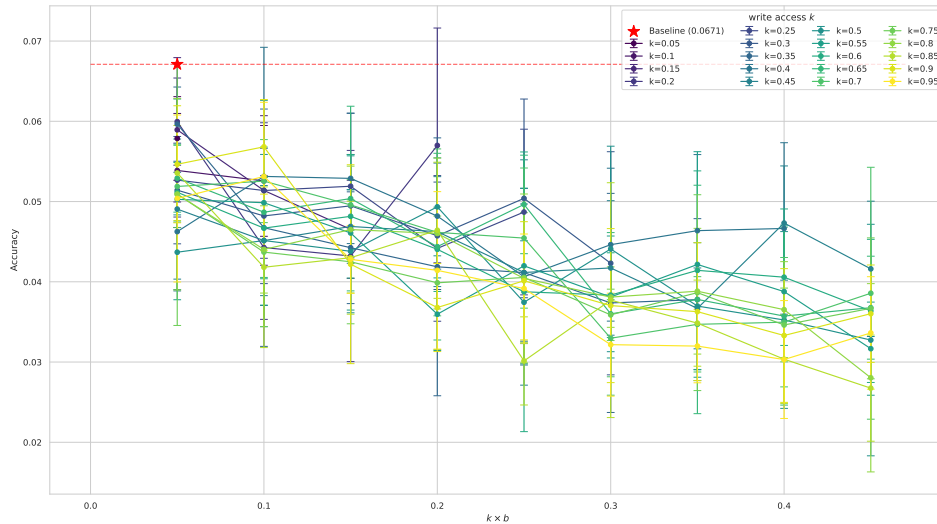


Figure 15: Logistic regression model on CIFAR100 dataset

918 CIFAR100 is very challenging for linear models, which explains the very low ($\approx 6\sim 7\%$) baseline
 919 accuracy. Despite this low ceiling, our attack still reduces accuracy in most settings. The degradation
 920 is smaller in absolute terms—again because there is little usable accuracy to destroy—but the trend
 921 across k remains visible: large write-access allows the attacker to consistently push gradients in
 922 harmful directions, even in high-class-count regimes.
 923

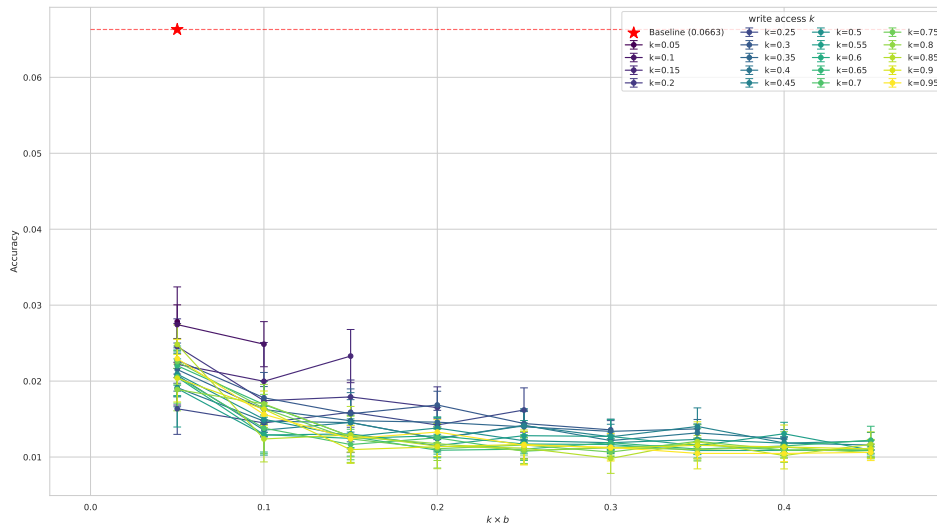


Figure 16: 2-layer vanilla MLP model on CIFAR100 dataset

944 As seen with CIFAR10, the attack again becomes more harmful than with a logistic regression. The
 945 same trend persists: generally, high write-access (k) settings produce the most damage, and the attack
 946 is efficient.

947 The following figure presents preliminary results demonstrating that our attack remains effective even
 948 on substantially larger and more expressive architectures. In particular, we evaluate the untargeted
 949 attack against a Vision Transformer trained on CIFAR-10. The observed accuracy degradation across
 950 different attacker budgets indicates that the vulnerability we study is not confined to linear or shallow
 951 models.
 952

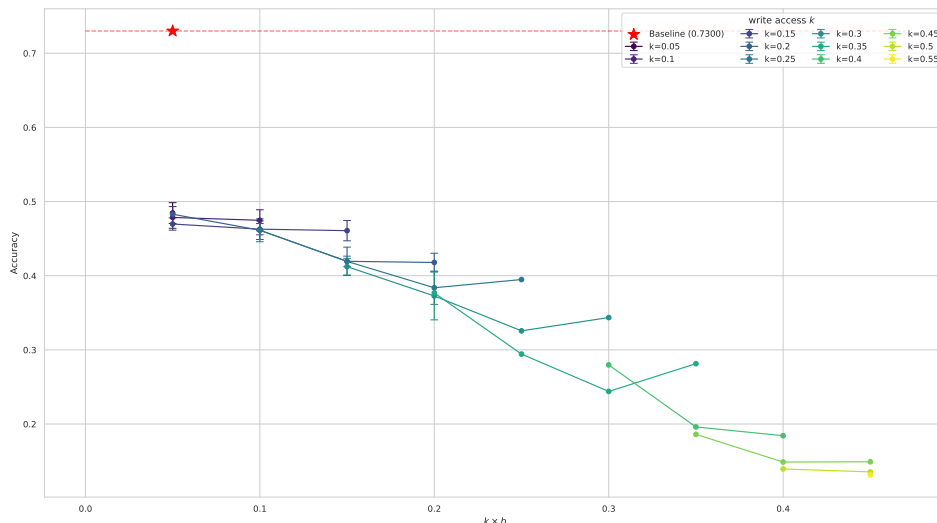


Figure 17: Vision Transformer (ViT_b_16) on CIFAR10 dataset

E ADDITIONAL EXPERIMENTS ON PERFORMANCE METRICS AND MODEL VARIATIONS

We provide additional results on the robustness of the models under different performance metrics and optimization strategies for the logistic regression on the Mnist dataset.

Figure 18 reports the F1 score as a function of the corrupted fraction $k \times b$. Similar to the test accuracy trends, the F1 score decreases steadily as the corruption level increases.

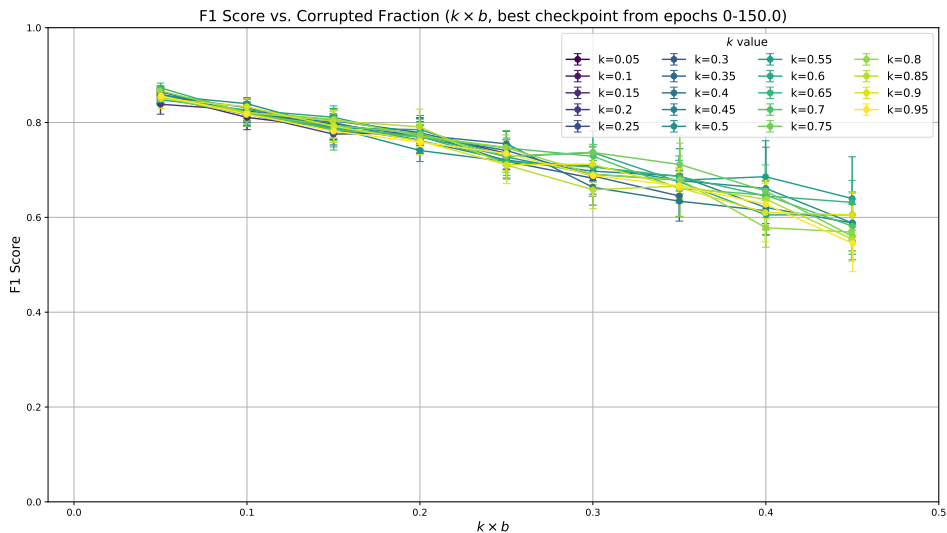


Figure 18: F1 score as a function of $k \times b$ with early stopping and an SGD optimizer.

So far, all results have used SGD optimization. We now contrast these findings with the Adam optimizer. Figure 19 seems to suggest that the attack is more effective with Adam compared to SGD.

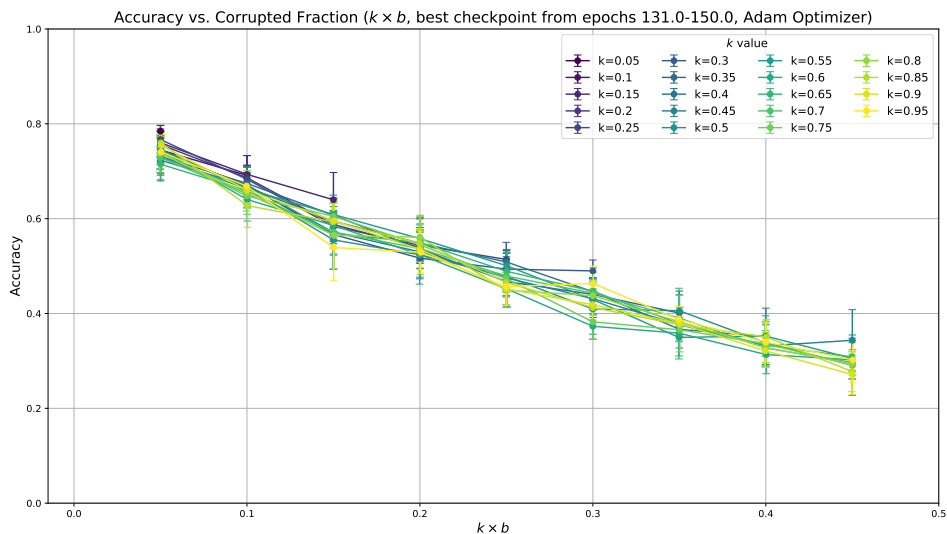


Figure 19: Adam optimizer: accuracy versus $k \times b$

F DETECTABILITY AND DATA NORMALIZATION.

In this section, we evaluate how detectable our label-flipping attack is under common feature-preprocessing pipelines, focusing on the gradient-norm statistics that many FL defenses monitor. Practical FL systems almost always apply some form of input normalization or scaling before training. Under these normalized settings, we empirically find that the attacker’s per-client gradient norms become nearly indistinguishable from those of honest clients (Table 3). As a result, defenses that rely solely on gradient-norm thresholds or magnitude-based outlier filtering are ineffective. In contrast, when data are left unnormalized, the attacker’s gradient norms may inflate (Table 4) which would make norm-based detection almost trivially successful.

Table 3: Normalized-data mean gradient-norm ratio (attacker mean gradient norm divided by honest mean gradient norm). Ratios extremely close to 1 indicate that, under standard dataset normalization, the attacker’s per-round gradient magnitudes are statistically indistinguishable from those of honest clients.

dataset	model	attack/honest norm ratio
cifar10	logreg	1.004523
cifar10	vanilla	1.000400
mnist10	logreg	1.028216
mnist10	vanilla	1.018608

Table 4: Unnormalized-data mean gradient-norm ratio. Without input normalization, the attacker’s gradient norms become significantly inflated, making simple norm-based defenses (e.g. clipping, outlier filtering) much more likely to detect the malicious client.

dataset	model	attack/honest norm ratio
cifar10	logreg	1.319266
cifar10	vanilla	1.333890
mnist10	logreg	7.306702
mnist10	vanilla	232.278825